Effect of Growth Solution Concentration on the Performance of Boron Doped ZnO Dye-sensitized Solar Cell (DSSC)

M.Y.A. Rahman[*,1], A.A. Umar[†,1], L. Roza[1], S.A.M. Samsuri[1], M.M. Salleh[1], I. Iwantono[2] and Tugirin[2]

[1]Institute of Microengineering and Nanoelectronics (IMEN), Universiti Kebangsaan Malaysia (UKM), Bangi, 43600, Selangor, Malaysia
[2]Department of Physics, Faculty of Mathematics and Natural Sciences, Universitas Riau, Pekanbaru, 28131, Indonesia

Abstract: *Synthesis parameter plays important role in modifying physical property of metal oxide films which serve as photoanode in dye-sensitized solar cell (DSSC). This paper reports the synthesis of boron doped ZnO nanostructures via seed mediated growth hydrothermal technique and their application as photanode in DSSC. The growth process was carried out at various solution concentrations, 0.1, 0.2, 0.3 and 0.4 M. The solution contains 1 % wt. dimethyl borate as boron source, hexamethylenetetramine (HMT) surfactant and zinc nitrate ($Zn(NO_3)_2$). The samples are crystalline with wurtzite phase. The morphological shape of the samples changes with the growth solution concentration. The optical absorption increases as the concentration increases. However, the band gap does not significantly change with the concentration. The DSSC utilizing the ZnO sample prepared at 0.1 M solution performs the best photovoltaic parameters with the J_{SC} of 0.969 mA cm^{-2}, FF of 0.48 and η of 0.222%, respectively since it shows the highest absorption and lowest photoluminescence in visible region.*

1. INTRODUCTION

Various efforts have been put in improving the performance of dye-sensitized solar cells (DSSCs) such as introducing core-shell structure onto photovoltaic materials [1,2], coated layer onto photovoltaic materials [3] and doping of photovoltaic materials [4-11]. Doping can be classified into non-metallic and metallic doping. The films are doped with these materials in order to modify the morphology and optical properties such as optical absorption and band gap energy. The morphology of photovoltaic material which also serves as photoanode influences the performance of DSSC [4-7]. The band gap of the films was lowered down, increasing the rate of free electron-hole pair and consequently improves the performance of the device [6-11]. The metallic doping materials that are widely utilized in DSSC are stannum doped ZnO [4], indium doped ZnO [5] and cerium doped TiO_2 [6]. While, the non-metallic doped materials are nitrogen doped TiO_2 [7-10], sulfur doped TiO_2 [7] and graphene doped TiO_2 [11].

It has been reported in [12] that boron doped ZnO thin film electrodes in DSSC was synthesized via spray pyrolysis technique. Boron doped ZnO as photoelectrode in DSSC synthesized via sol-gel technique has been reported in [13]. The boron source was acid boric [12,13]. In this work, we have introduced another source of boron that is dimethyl borate which is added into a growth solution containing $Zn(NO_3)_2$ and HMT via hydrothermal technique. The objective of the work is to investigate the influence of growth solution concentration on the structure, morphology, thickness, elemental composition, optical absorption and band gap of ZnO nanotubes. These properties are related to the performance parameters of the DSSC utilizing the ZnO samples.

2. EXPERIMENTAL

The ZnO nanostructures were grown on FTO substrate via simple seed mediated hydrothermal technique. This method involved 2 route steps, namely, seeding process by deposition of ethanolic zinc acetate dihydrate to prepare uniforms ZnO nanoseed and followed by the growth process in aqueous solution containing dimethyl borate, zinc nitrate hexahydrate ($Zn(NO_3).6H_2O$) and hexamethylenetetramine (HMT). Reagent grade of dimethyl borate,

---

To whom correspondence should be addressed:
*mohd.yusri@ukm.edu.my, †akrajas@ukm.edu.my

$Zn(NO_3).6H_2O$ and HMT powders ($\geq$ 99.0% in purity) were used without any purification. Before seeding process, the substrates were cleaned using a standard cleaning procedure in acetone, 2-propanol and ethanol for 15 minutes in ultrasonic bath, respectively. The substrates were then dried under nitrogen flow. After the cleaning treatment, the substrates were used immediately for growth process.

2.1. Seeding Process

ZnO nanoseeds on the FTO surface were prepared using an alcohol-thermal seeding method. A thin layer of ethanolic solution of 10 mM zinc acetate dihydrate ($Zn(CH_3COO)_2\,2H_2O$) on a cleaned FTO surface was firstly prepared by two-steps spin-coating process for 6 seconds at 400 rpm and followed for 30 seconds at 3000 rpm to make sure the solution was evenly distributed on the substrate and to get the sufficient thickness of the seed growth on the substrate. The sample was then dried at 100 ^{o}C on a hot-plate for 15 minutes and then cooled down to 60 ^{o}C. These procedures were repeated three times in order to get appropriate thickness of ZnO nanoseeds. The sample was annealed at 350 ^{o}C for 1 hour in air condition, using a horizontal tube furnace.

2.2. Growth Process

The sample was subsequently immersed in a growth solution. The growth of ZnO nanostructures from the nanoseeds was carried out by immersing the nanoseeds-attached FTO in a equimolar solution, 0.1 M of $Zn(NO_3).6H_2O$ and HMT. Then, 1 % wt. dimethyl borate was added into the solution and the growth reaction was carried out at 90 ^{o}C for 8 h inside an electric oven. The substrate with ZnO seed layer was put face down in the growth solution. After heating for 8 h at 90 ^{o}C, the solution was subsequently cooled down to 50 ^{o}C and the reaction was left for 16 h. After the growth process, the samples were then taken out and washed several times using pure water in order to remove any precipitation on their surface and dried using a flow of nitrogen gas for characterizations. These procedures were repeated for preparing the samples with 0.2, 0.3 and 0.4 M solutions.

The structure and phase structure of the samples were examined by X-ray diffraction (XRD) model Bruker D8 Advance. The morphology of the ZnO nanostructures was observed using field-emission scanning electron microscopy (FESEM) analysis (Zeiss Supra 55VP FESEM) with the magnification of 50000×. The outer diameter of the ZnO nanotubes was estimated by using the scale located at the lower corner of the FESEM images. The thickness of the nanotubes was estimated from the cross-sectional image of the FESEM. Energy dispersive x-ray (EDX) spectrometer was employed for the elemental analysis. Optical spectrophotometer UV–Vis Lambda 900 Perkin Elmer was employed to study the optical absorption and reflectance of the ZnO samples. Photoluminescence spectrophotometer was employed to study the photoluminescence of the samples.
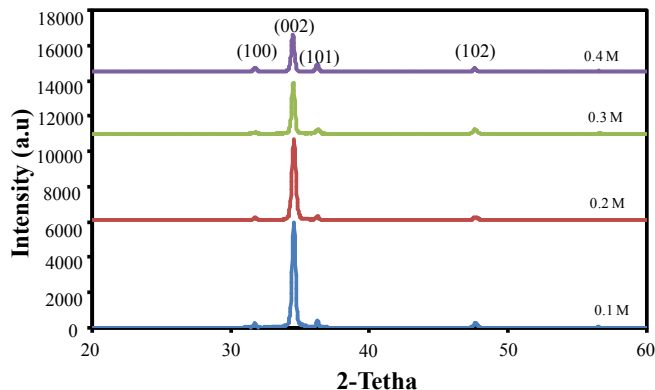

Figure 1. XRD spectra of the ZnO samples with various growth solutions doped with 1% boron

2.3. Fabrication and performance study of DSSC

The boron doped ZnO samples were immersed into an ethanolic solution of 0.3 mM N719 dye for 2 h. The dipping time above 2 hours can be used since it will etch the ZnO films on the substrate. The samples were then taken out, rinsed gently with fresh ethanol and then dried under a flow of nitrogen gas. Platinum film as a counter electrode was prepared by depositing plastisol on the FTO substrate. An electrolyte containing 0.5 M LiI/0.05 M I_2/0.5 M TBP in acetonitrile was used as a redox couple. A DSSC was fabricated by sandwiching the parafilm between the ZnO samples and platinum counter electrode. The electrolyte was injected into the cell and filled via a capillary. The performance study of the cell was carried out by observing the current–voltage in the dark and under illumination using an AM 1.5 simulated light with an intensity of 100 mW cm^{-2}. The illuminated area of the cell was 0.23 cm^2. The current–voltage curves in the dark and under illumination were recorded by a Keithley high-voltage source model 237 interfaced with a personal computer.

3. RESULTS AND DISCUSSION

Fig. 1 shows the XRD patterns of ZnO samples with various concentrations of the growth solution. The diffraction patterns show three wurtzite phase peaks at 33.90^o, 36.39^o, 37.20^o and 47.48^o, respectively [14]. According to the JCPDS (file no.36-1451), the peaks are attributed to (100), (002), (101) and (102) plane, respectively. It is noticed that the peak intensity at (002) decreases with the growth concentration. This is due to thickness of the sample increases with the concentration as presented in Table 1. With the increase in the thickness, the X-ray signal penetrating the sample becomes weaker. The height of peak intensity at other planes is about the same. It is also found that the full width half maxima (FWHM) of the peak at (002) plane does not significantly

Table 1. Energy gap, thickness and photovoltaic parameter of the cell utilizing ZnO samples grown at various concentrations

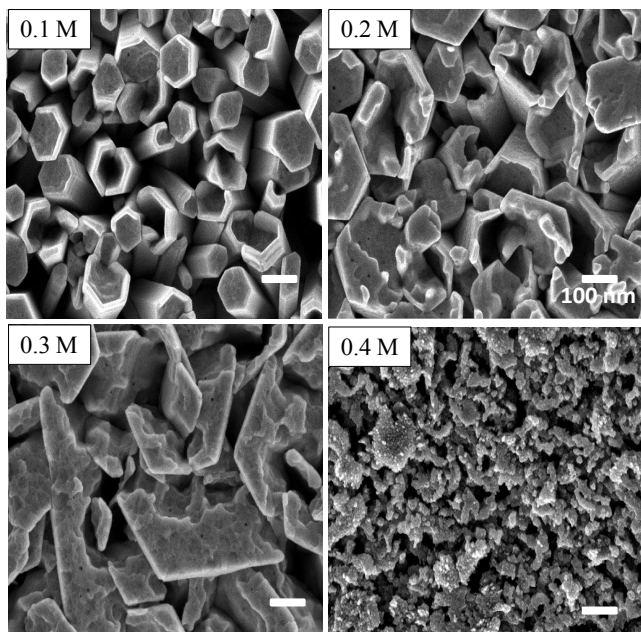| Growth solution (M)	Energy gap (eV)	Thickness (μm)	V_{OC} (V)	J_{SC} (mA cm^{-2})	FF	η (%)
0.1	3.11	1. 68	0.48	0.969	0.48	0.222
0.2	3.11	2.42	0.54	0.796	0.36	0.156
0.3	3.10	3.19	0.46	0.319	0.37	0.054
0.4	3.10	3.56	0.54	0.564	0.15	0.148

Figure 2. FESEM images of ZnO samples of various growth solution concentrations
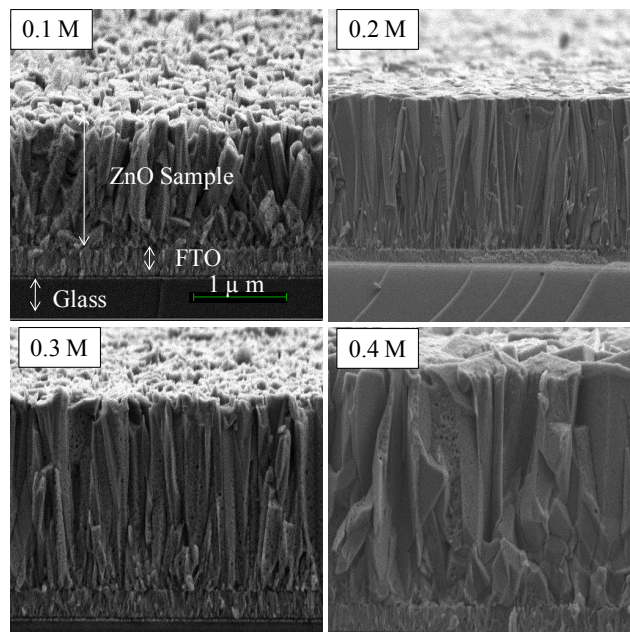

Figure 3. FESEM cross-sectional images of the ZnO nanotubes synthesized at various growth concentrations
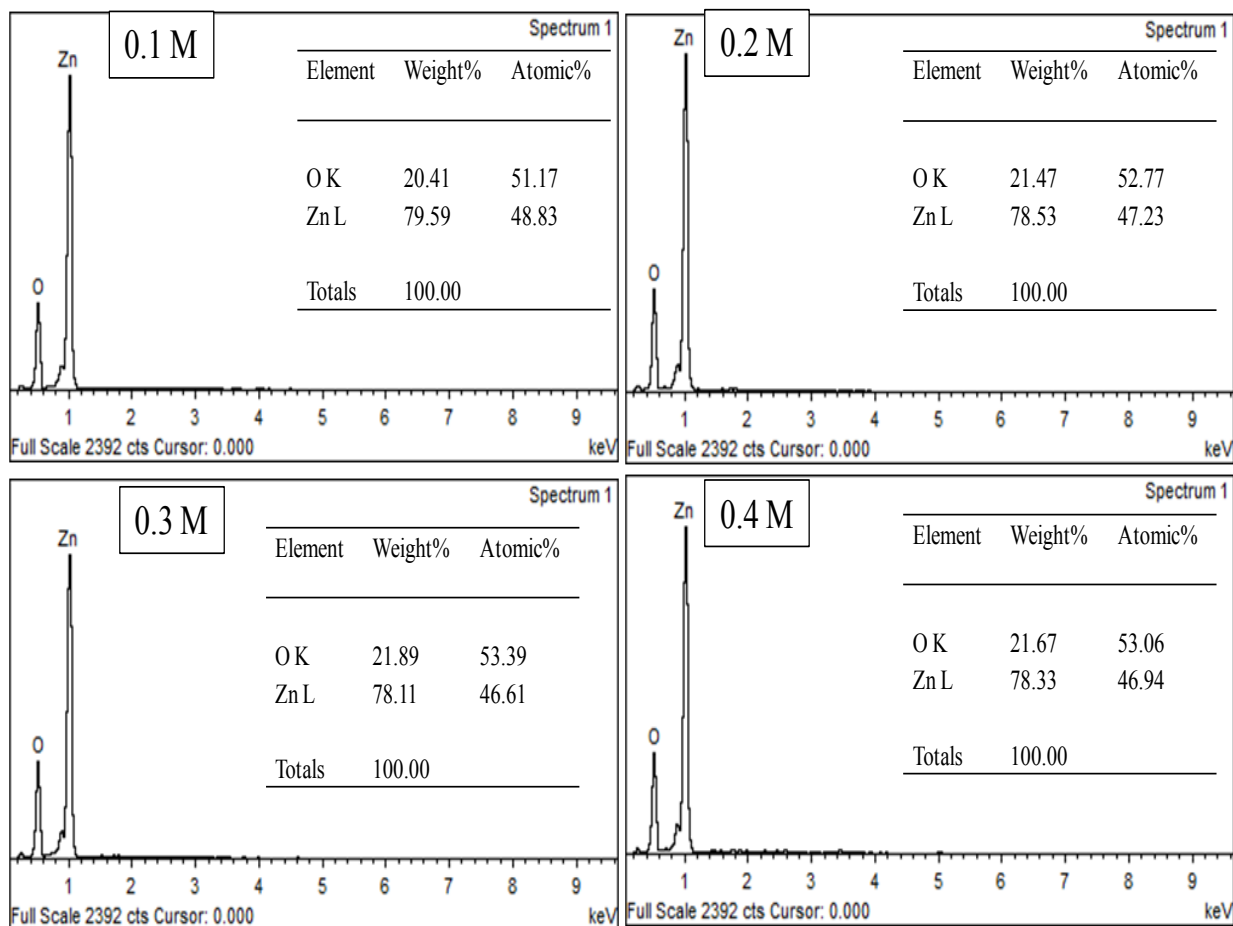

Figure 4. EDX spectra of the samples with various growth solution concentrations
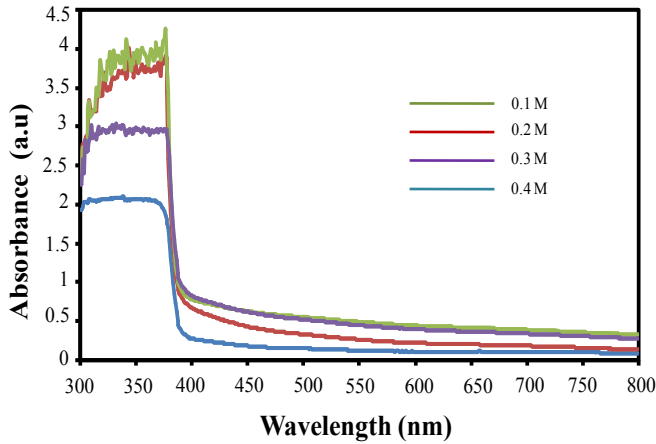
Figure 5. UV-VIS optical absorption spectra of ZnO nanostructure with different growth solution concentrations
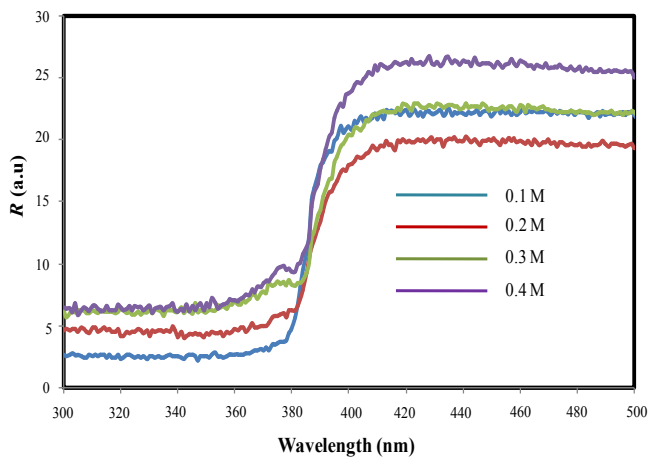

Figure 7. Tauc plots with various growth solution concentrations

Figure 6. Reflectance spectra with various growth solution concentrations
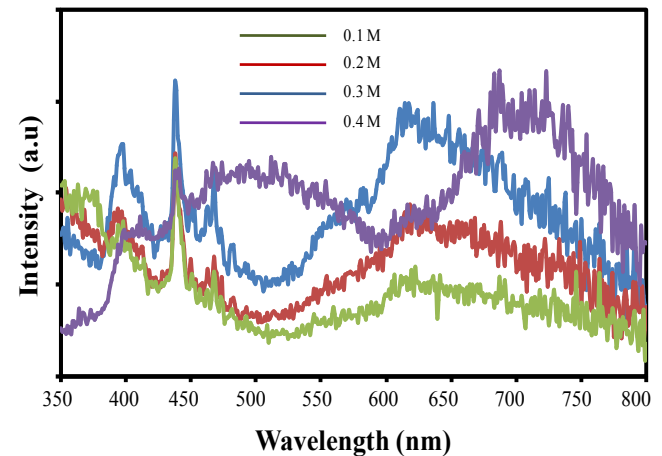
Figure 8. Photoluminescence spectra of ZnO samples prepared at various growth solution concentrations

change with the concentration. According to Scherrer formula, the crystallite size of the sample is about the same.

Fig. 2 shows the FESEM images of the ZnO nanotubes synthesized at various growth solution concentrations. It is obviously seen from the images that the morphology of the samples changes with the concentration. The shape of nanostructure is irregular for 0.2, 0.3 and 0.4 M samples. At 0.1 M, the morphological shape of mixture of nanotubes and nanorods is observed. However, at 0.2 M, the nanostructure becomes cracked. The average diameter for 0.1 M sample is 110 ±10 nm. The shape is transformed into nanoplate when the concentration is further increased to 0.3 M. The morphology is then changed into cracked-nanoplate at 0.4 M concentration.

Fig. 3 shows the FESEM cross-sectional images of the samples synthesized at various growth concentrations. From the images, it is found that the ZnO nanostructure layer is formed on FTO substrate for each sample. The thickness of the samples is illustrated in Table 1. From the table, it is observed that the thickness increases with the concentration of the growth solution.
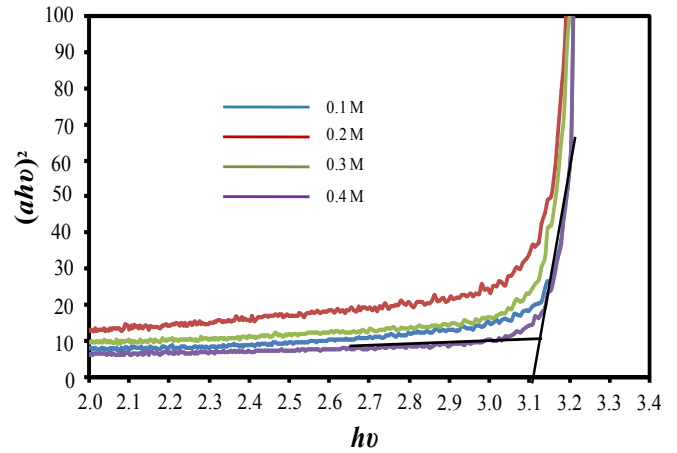
Fig. 4 illustrates the EDX spectra for ZnO nanotubes with various concentrations of the growth solution. As the concentration increases, the oxygen weight and atomic percentage increases but those of zinc decrease until the concentration of 0.3 M. At 0.4 M, the weight and atomic percentage of oxygen decreases. On the other hand, those of zinc increase. This phenomenon is normal since if the weight and atomic percentage of a particular element increase, those of another element also decrease.

Fig. 5 shows the optical absorption spectra of ZnO samples prepared at various growth solution concentrations. The UV-Vis spectra of all samples show quite similar pattern. The curves show strong absorption at the wavelength less 390 nm and weak absorption after 390 nm in the range from visible to near infrared. It is noticeable the absorption of the sample decreases with the concentration of growth solution. The 0.1 M sample shows the highest absorption, while the 0.4 M sample possesses the lowest absorption since it has the smallest particle size. The particles with smaller size absorb less light than those with bigger size [15].

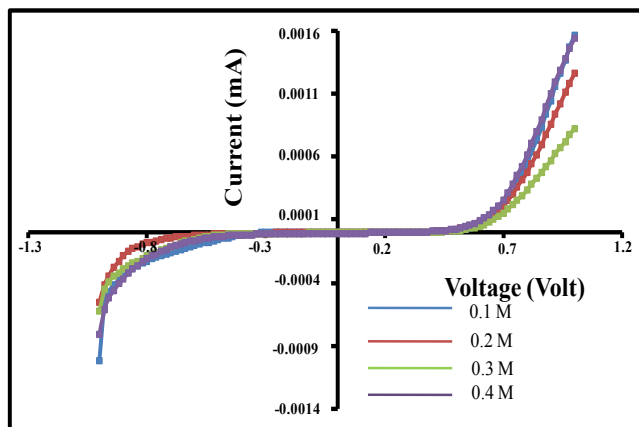Fig. 6 shows the reflectance spectra of ZnO samples prepared at

Effect of Growth Solution Concentration on the Performance of Boron Doped ZnO Dye-sensitized Solar Cell (DSSC)
/ J. New Mat. Electrochem. Systems

217

Figure 9. Dark current of the DSSC with various precursor concentrations
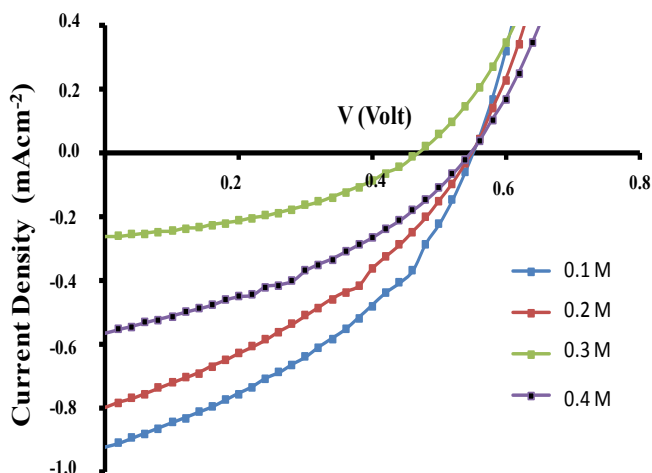

Figure 10. *J-V* curves of the cells utilizing the ZnO samples with different concentration of growth solution under 100 mW cm^{-2} light illumination

various growth solution concentrations. The spectra of all samples show similar pattern. The curves show strong reflection at the wavelength above 390 nm and weak reflectance below 390 nm. It is noticeable the absorption of the sample increases with the concentration of growth solution. The 0.1 M sample shows the lowest reflection, while the 0.4 M sample possesses the highest reflection. These results are opposite to those of absorption. In other word, higher absorption, lower reflection and vice-versa. The reflectance spectra in Fig. 6 are transformed into Tauc plots presented in Fig. 7. From the figure, it is found that the energy gap of the sample listed in Table 1 does not significantly change with the growth solution concentration. It is concluded that the concentration does not affect the energy gap of ZnO.

Fig. 8 shows the photoluminescence (PL) spectra of ZnO samples prepared at various growth solution concentrations. The sample with 0.3 M possesses the highest photoluminescence peak, followed by 0.2, 0.1 and 0.4 M sample at 390 and 440 nm. The

range between these wavelengths is in visible region. These results indicate that the 0.3 M sample has the highest rate of recombination between electron and hole, followed by 0.2, 0.1 and 0.3 sample. In other words, the 0.2 M sample exhibits the highest excitonic state, followed by 0.2, 0.1 and 0.3 M sample. However, the 0.1 M sample shows the lowest PL in the visible region, ranging from 400-450 nm. The excitonic state is also called the bound state of electron and hole. The PL spectra patterns shown in this figure are quite similar to those reported in [16].

Fig. 9 shows the *I-V* curves under dark condition of the DSSCs utilizing the ZnO sample synthesized at various concentrations of the growth solution. It is noticed from the figure that the devices do not show rectification property since the dark current in the reverse is about the same with that in the forward bias. However, the device allows quite high dark current in both biases which is in the mA range. For both biases, the different in the current for all devices is also small indicating that the concentration of the growth solution does not influence the dark current.

Fig. 10 shows the *J-V* curves of the DSSC utilizing the ZnO samples prepared with various concentrations of the growth solution under 100 mW cm^{-2} light illuminations. The device with 0.1 M concentration generates the highest output power, while the device with 0.3 M concentration demonstrates the lowest output power. The slope of each curve is quite high, indication of high internal resistance of the devices, leading to small fill factor (*FF*). The photovoltaic parameters are illustrated in Table 1. According to the table, it was found that the device with 0.1 M concentration demonstrates the highest J_{SC} and η. This is due to this device possesses the highest optical absorption and the lowest photoluminescence as illustrated in Fig. 4 and Fig.8, respectively. There is no significant change in V_{OC}. Generally, from Table 1, the fill factor is low since the area of maximum power rectangles drawn from the *J-V* curves is much smaller than that of the *J-V* curves. This is due to high power loss which is caused by high leakage current in the device as illustrated in the *I-V* curves in dark presented in Fig. 9. The highest η produced from this work is smaller than that reported in [17] which was 0.29%. The boron source was boric acid. It is much smaller than those reported in [12, 13] which were 1.53% and 1.56%, respectively. The low efficiency of the DSSC fabricated in this work is due to the dipping time of boron doped ZnO samples into N719 dye solution is insufficient, resulting in low optical absorption of the ZnO sample.

4. CONCLUSIONS

The element of boron was successfully doped into the ZnO films by adding dimethyl borate into the growth solution containing $Zn(NO_3).6H_2O$ and HMT. The optical absorption of ZnO nanotubes decreases as the growth solution concentration increases. The DSSC utilizing ZnO nanotubes prepared at 0.1 M concentration demonstrates the highest J_{SC} and η of 0.969 mA cm^{-2} and 0.222%, respectively. The highest performance of the device utilizing the ZnO nanotube prepared 0.1 M possesses the highest optical absorption and lowest photoluminescence in visible region.

5. ACKNOWLEDGMENTS

REFERENCES

[1] Law M, Greene LE, Radenovis A, Kuykendall T, Liphardt J, Yang P, J Phys Chem B, 110, 22652 (2006).

[2] Samsuri SAM, Rahman MYA, Umar AA, Salleh MM, J Mat Sci., Mat Elect., 26, 4936 (2015).

[3] Karuppuchamy S, Nonomura K, Yoshida T, Sugiura T, Minoura H, Sol State Ion., 151, 19 (2002).

[4] Ameen S, Akhtar MS, Seo H-K, Kim YS, Shin HS, Chem Eng J., 187, 351 (2012).

[5] Tubtimtae A, Lee M-W, Superlatt Microstruc., 52, 987 (2012).

[6] Zhang J, Peng W, Chen Z, Chen H, Han L, J Phys Chem C, 116, 19182 (2012).

[7] Zhang JC, Han ZY, Li QY, Yang XY, Yu Y, Cao WL, J Phys Chem Sol., 72, 1239 (2011).

[8] Rahman MYA, Umar AA, Saad SKM, Salleh MM, Ishaq A, J New Mater Electrochem System., 17, 33 (2014).

[9] Ma T, Akiyama M, Abe E, Nano Letter, 5, 2543 (2005).

[10]Lim CK, Huang H, Chow CL, Tan PY, Cheng X, Tse MS, Tan OK, J Phys Chem C, 116, 19659 (2012).

[11]Tang Y-B, Lee C-S, Xu J, Liu Z-T, Chen Z-H, He Z, Cao Y-L, Yuan G, Song H, Chen L, Luo L, Cheng H-M, Zhang W-J, Bello I, Lee S-T, ACS NANO, 4, 3482 (2010).

[12]Pawar BN, Cai G, Ham D, Mane RS, Ganesh T, Ghule A, Sharma R, Jadhava KD, Han SH, Solar Energy Mater Solar Cells, 93, 524 (2009).

[13]Kumar V, Singh N, Kumar V, Purohit LP, Kapoor A, Ntwaeaborwa OM, Swart HC, J App. Phys, 114, 134506 (2013).

[14]Rusdi R, Rahman A, Mohamed NS, Kamarudin N, Kamarulzaman N, Powder Tech, 210, 18 (2011).

[15]Iwantono I, Nurwidya W, Lestari LR, Naumar FY, Nafisah S, Umar AA, Rahman MYA, Salleh MM, J Solid State Electrochem, 19, 1217 (2015).

[16]Roza L, Rahman MYA, Umar AA, Salleh MM, J Alloys Comp, 618, 153 (2015).

[17]Rahman MYA, Roza L, Umar AA, Salleh MM, J Alloys Comp., 648, 86 (2015).